CONF-880534--11

DE88 016886

THE ICRF ANTENNAS FOR TFTR*

D.J.Hoffman, P.L. Colestock,† W.L. Gardner, J.C. Hosea,† A. Nagy,† J. Stevens,† D.W. Swain, J.R. Wilson†

Oak Ridge National Laboratory, Oak Ridge, Tennessee 37831, U.S.A.

Two compact loop antennas have been designed to provide ion cyclotron resonant frequency (ICRF) heating for TFTR. The antennas can convey a total of 10 MW to accomplish core heating in either high-density or high-temperature plasmas. The near-term goal of heating TFTR plasmas and the longer-term goals of ease in handling (for remote maintenance) and high reliability (in an inaccessible tritium tokamak environment) were major considerations in the antenna designs. The compact loop configuration facilitates handling because the antennas fit completely through their ports. Conservative design and extensive testing were used to attain the reliability required for TFTR. This paper summarizes how these antennas will accomplish these goals.

The Antenna Designs

Two antennas have been designed, fabricated, tested, and installed on TFTR. One antenna, built by Princeton Plasma Physics Laboratory, is designed to couple 6 MW for 2 s at 47 MHz through the 74- by 90-cm Bay M port; the other, built by Oak Ridge National Laboratory, is designed to couple 4 MW through the 60- by 90-cm Bay L port. Figure 1 shows the layout of the Bay L antenna; Fig. 2, the layout of the Bay M antenna. Each antenna can be installed through its port and can move ≈10 cm relative to the plasma. Each one has a pair of current straps that can be independently phased to control the launched k spectrum. Both will operate at CIT-level power densities (on the Faraday shield) of ≈1.2 kW/cm^2.

Although the antennas were principally constructed for core heating of a hot, dense plasma, they were also intentionally designed with different features to provide experience in optimizing antenna design on future machines like CIT. One Faraday shield was built so that its TiC-coated elements would be relatively warm during operation; the other shield's graphite-covered elements will be actively cooled. Designs for CIT antennas call for matching by either stubs or capacitive structures. To help resolve this issue, one antenna is matched by variable capacitors at both ends of the current strap and is fed centrally. With properly chosen capacitance values, the antenna can be made to have a 50-Ω impedance at the feed point. This antenna is tunable from 35 to 68 MHz on the presently installed structure and can be modified without breaking vacuum for 60- to 80-MHz operation. The other antenna is end-fed, with all matching accomplished by external stubs. By phasing the feed lines, each strap can be made to operate as a magnetic dipole or quadrupole. The differences between the two configurations are summarized in Table I.

*Research sponsored by the Office of Fusion Energy, U.S. Department of Energy, under contract DE-AC05-84OR21400 with Martin Marietta Energy Systems, Incorporated.

†Princeton Plasma Physcis Laboratory, Princeton, New Jersey 08544, U.S.A.

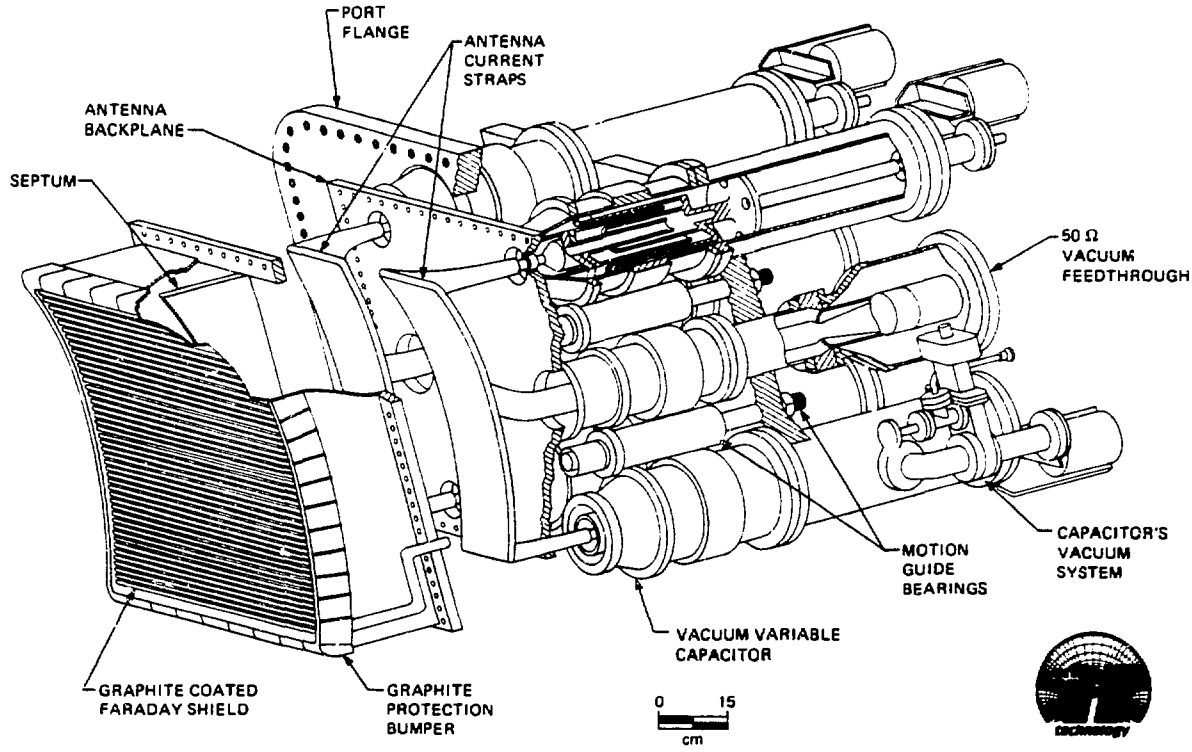

Fig. 1. The Bay L antenna.

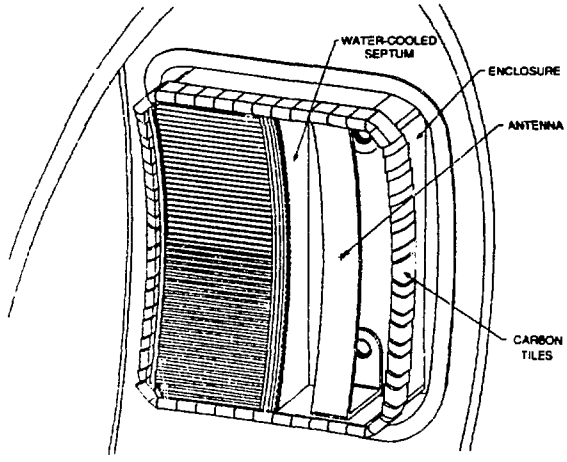

Fig. 2. The Bay M antenna.

Table I. Bay L and Bay M antenna characteristics

	Bay L	Bay M
Total power (MW)	4	6
Frequency (MHz)	40–60	47
Pulse length (s)	2	2
RF material	Copper	Silver
Matching		
Location	Internal	External
Method	Capacitors	Stubs
Current strap impedance (Ω)	62	40
Relative phase velocity (%)	81	43
Feed point	Central	End
Number of straps per port	2	2
Port size (cm × cm)	60 × 90	74 × 90
Shield power density (kW/cm²)	1.2	1.2
Antenna motion (cm)	11	11
Faraday shield		
Coating	Graphite	TiC
Material	Inconel 625	Inconel 625
Cooling	Active	Inertial
Side wall configuration	Closed	Slotted

Power Considerations

To couple all of the power, either relatively high-voltage, high-current capabilities or high loading is required. The compact loop configuration helps to increase loading by permitting the backplane to be almost totally recessed. Both antennas have this feature. To quantify the effect, the backplane is placed 20 cm (instead of 4 cm, as an internally mounted antenna might require) from the current strap in the Bay L coupler, which increases the plasma flux linkage a factor of 2. To further increase the coupling of the Bay M antenna, the antenna sidewalls are slotted, which improves coupling by a factor of 5 during in-phase operation. The Bay L antenna sidewalls are closed to prevent plasma penetration, but coupling modestly improves (1.2 times) during out-of-phase operation. Both antennas have high flux linkage and should have better coupling than antennas with close backplanes. The voltage and current requirements for full power, shown in Figs. 3 and 4 as functions of distributed plasma load, are similar for the two antennas. For the Bay L coupler, the slight electrical asymmetries in the circuitry and different strap impedance give curves different from those for Bay M. At the rated voltage of 50 kV peak, the efficiency of the antenna with the graphite Faraday shield is 96%; of the antenna with the TiC shield, 98%.

Testing

Both antennas were subjected to numerous tests to prove that they would operate reliably in TFTR: disruption thermal load tests of the Faraday shield elements, mechanical tests of the vacuum feedthroughs, bakeout tests, other miscellaneous tests, and high-voltage tests of the entire assembly. The last are the most important in

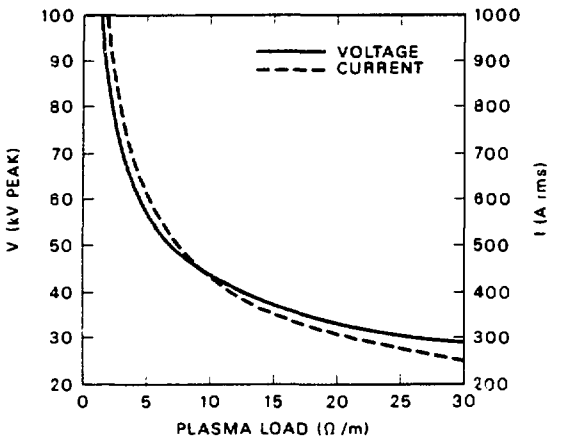

Fig. 3. Maximum capacitor voltage and current versus plasma load in the Bay L antenna, assuming 2 MW per strap at 47 MHz. The capacitors must vary as a function of plasma load and slightly change the site of current maximum. As a result, the curves do not follow a simple, distributed coaxial transformation.

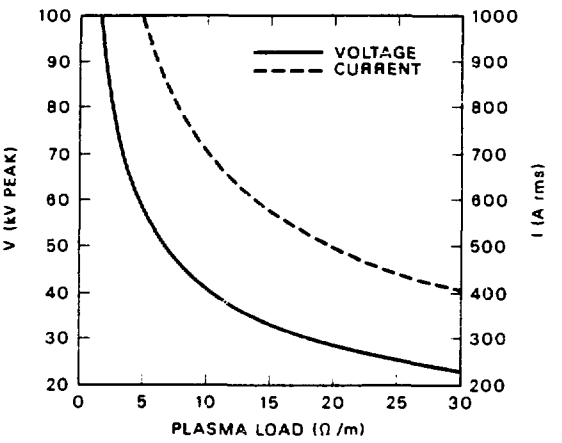

Fig. 4. Maximum strap voltage (at the feedthrough) and current (in the midplane) versus plasma load in the Bay M antenna, assuming 3 MW per strap at 47 MHz. This antenna follows the coaxial transformation.

qualifying the assemblies for high-power operation. Both structures were subjected to high-voltage, long-pulse tests in a variety of environments, including vacuum, gas, magnetic fields, and plasmas. Especially after the antennas were baked out, none of these items degraded the antennas' voltage capabilities. Both made reliable 2-s, 47-MHz pulses at 65 kV peak. This exceeds the 50-kV design value.

Spectral Considerations for Heating in TFTR

The spectral design of the antennas must accommodate good plasma heating and the constraints imposed by the ports. The larger port sets the lower limit of $k \approx 4\ \mathrm{m}^{-1}$. However, calculations for TFTR indicate that central ion heating is peaked around $k \approx 10\ \mathrm{m}^{-1}$. Figure 5 shows that the outgoing wave damps over 40% of the power on the ^{3}He minority in the core on the first pass. This case is for 47 MHz, $6 \times 10^{13}\ \mathrm{cm}^{-3}$, 5% minority in a high-$T_i$ deuterium plasma. Virtually no power is damped directly on the electrons. Thus, the antennas were designed with two current straps per port to generate $k \approx 10\ \mathrm{m}^{-1}$ in Bay M. The smaller port in Bay L restricts the out-of-phase spectrum to be centered on $15\ \mathrm{m}^{-1}$, well within the spectral peak of ion heating. Since TFTR runs under a variety of conditions, including dense hydrogen discharges, the achievable range of k is from $4\ \mathrm{m}^{-1}$ to $15\ \mathrm{m}^{-1}$. This, combined with the frequency range of the antennas, will ensure that ion heating is accomplished.

Conclusions

The antennas for TFTR have been optimized to heat the hot, dense plasma. Intentional differences have been designed into the two antennas to help selection of important features for future heating experiments on TFTR or CIT.

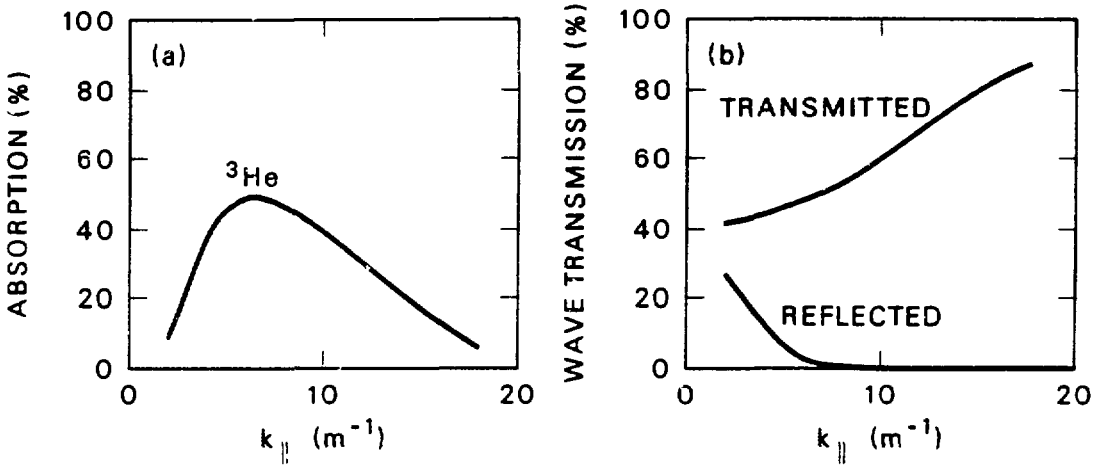

Fig. 5. (a) Wave damping on the ^{3}He minority as a function of $k_\parallel$. The absorption from the high-field side is virtually the same as that from the low-field side. (b) Propagation of the wave through TFTR. Little reflection is seen.

DISCLAIMER